

See discussions, stats, and author profiles for this publication at: <https://www.researchgate.net/publication/260642904>

Assembly of a Chiral Amino Acid on an Unreactive Surface: (S)-Proline on Au(111)

ARTICLE *in* LANGMUIR · MARCH 2014

Impact Factor: 4.46 · DOI: 10.1021/la500336c · Source: PubMed

CITATIONS

2

READS

68

8 AUTHORS, INCLUDING:



Federico Grillo

University of St Andrews

17 PUBLICATIONS 226 CITATIONS

[SEE PROFILE](#)



Stephen M Francis

University of St Andrews

42 PUBLICATIONS 761 CITATIONS

[SEE PROFILE](#)



Renald Schaub

University of St Andrews

27 PUBLICATIONS 2,317 CITATIONS

[SEE PROFILE](#)



Christopher J Baddeley

University of St Andrews

94 PUBLICATIONS 2,299 CITATIONS

[SEE PROFILE](#)

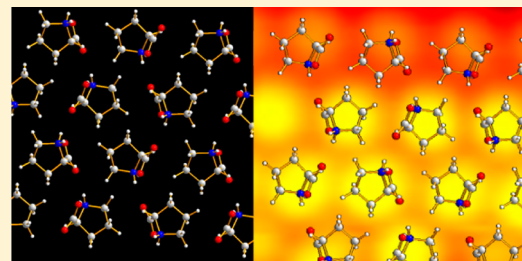
Assembly of a Chiral Amino Acid on an Unreactive Surface: (S)-Proline on Au(111)

Riho T. Seljamäe-Green,[†] Grant J. Simpson,[†] Federico Grillo,[†] John Greenwood,[†] Stephen M. Francis,[†] Renald Schaub,[†] Paolo Lacovig,[‡] and Christopher J. Baddeley^{†,*}

[†]EaStCHEM School of Chemistry, University of St Andrews, St Andrews, Fife, KY16 9ST, United Kingdom

[‡]Elettra-Sincrotrone Trieste S.C.p.A., Strada Statale 14 Km 163.5, Trieste I-34149, Italy

ABSTRACT: The adsorption of (S)-proline on Au(111) at 300 K was studied by low-temperature scanning tunnelling microscopy, X-ray photoelectron spectroscopy, and high resolution electron energy loss spectroscopy. (S)-proline adsorbs to produce a 2-D gas phase at 300 K, which can be condensed to form ordered molecular assemblies on cooling to 77 K. The chemical nature of the self-assembled structures is discussed in light of the information provided by photoelectron and vibrational spectroscopies.



INTRODUCTION

The interaction of amino acids with surfaces has attracted considerable interest in recent years. As fundamental biomolecular building blocks, amino acids provide excellent model systems for the development of biosensors,¹ molecular electronics,^{2,3} or for understanding the interactions of biomaterial with artificial implants in medical applications.^{4,5} In addition, as readily available chiral molecules, amino acids have been used as chiral modifiers in enantioselective heterogeneous catalysis.⁶

So far, most studies of amino acid adsorption have focused on single crystal surfaces of relatively reactive substrates, such as Cu(110),^{7–25} Pd(111),^{26–28} Ni(111),^{29–31} and TiO₂(110).^{5,32–36} Extensive studies have been reported of sulfur containing amino acids such as cysteine^{37–39} and methionine⁴⁰ on Au(111) where the relatively strong Au–S bond drives the formation of chemisorbed species. There are fewer studies of non-sulfur containing amino acids. The amino acids tend to form physisorbed layers giving rise to 2-D gases.⁴¹ Nonetheless, it has been reported that physisorbed glycine restructured the Au(110)–(1 × 2) surface.⁴¹ In addition, Wilson et al. demonstrated the formation of ordered islands of (S)-lysine ($\text{NH}_2(\text{CH}_2)_4\text{CH}(\text{NH}_2)\text{COOH}$) on Au(111) and showed that lysine interacts sufficiently strongly with the Au surface to induce restructuring of the surface and the formation of highly oriented nanofingers.⁴²

Proline is of particular interest due to its unique structure among naturally occurring amino acids with a secondary α -amino group that is fused within a 5-membered ring imposing considerable constraints on the flexibility of the molecular structure (Figure 1). The cyclic backbone reduces the degree of conformational freedom of the molecule, which is important in protein chemistry where proline is utilized in biological systems to produce highly kinked tertiary protein structures. This lack

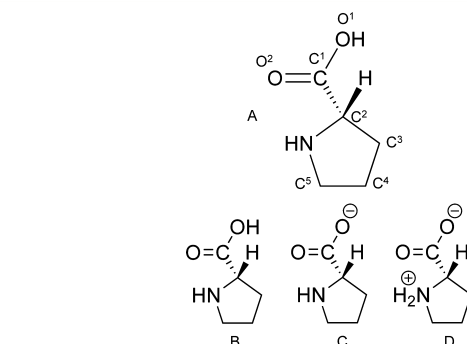


Figure 1. Molecular structures of (S)-proline. (A) with C and O atoms labeled to aid with interpretation of XPS data; (B) the neutral (non-zwitterionic) form; (C) the anionic form; and (D) the zwitterionic form of (S)-proline.

of conformational freedom was also found to influence the adsorption footprint of proline on the Cu(110) surface.^{17,43–45}

In this investigation, we use X-ray photoelectron spectroscopy (XPS), low temperature scanning tunneling microscopy (STM), and high resolution electron energy loss spectroscopy (HREELS) to probe the adsorption of (S)-proline on Au(111). We show that proline adsorption at 300 K occurs as a mixture of the zwitterionic, neutral, and anionic molecular forms and that ordered molecular arrangements are formed when the sample is cooled to 77 K.

EXPERIMENTAL SECTION

Low Temperature–Scanning Tunneling Microscopy (STM). All experiments were performed in a UHV surface analysis system with

Received: January 24, 2014

Revised: March 3, 2014

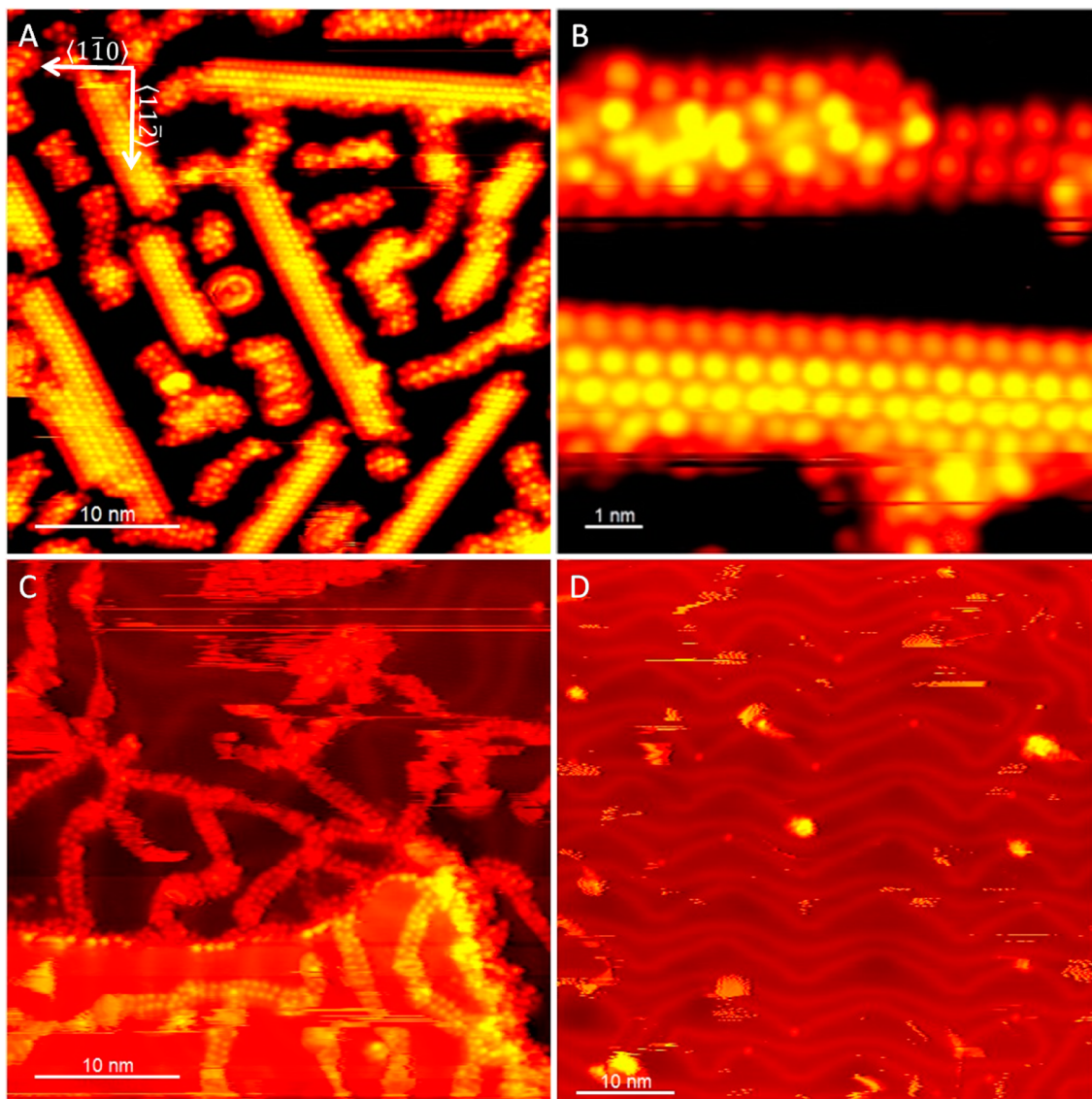


Figure 2. STM images acquired at 77 K after the Au(111) sample was exposed to (S)-proline at 300 K. (A) $37.5 \times 37.5 \text{ nm}^2$, 0.47 V, 0.03 nA; (B) $9.4 \times 9.4 \text{ nm}^2$, 0.47 V, 0.03 nA; (C) Annealed to 340 K, $37.5 \times 37.5 \text{ nm}^2$, -0.87 V, 0.02 nA; and (D) annealed to 370 K, $55.1 \times 55.1 \text{ nm}^2$, -1.29 V, 0.02 nA.

a base pressure below 1×10^{-10} mbar consisting of a preparation chamber allowing for standard sample preparation and a microscope chamber housing a CreaTec low-temperature STM. STM was performed at 77 K in constant-current mode utilizing homemade PtIr tips.

High Resolution Electron Energy Loss Spectroscopy (HREELS). HREELS measurements were carried out using a VSW HIB 1000 double pass spectrometer mounted on a UHV chamber working with a base pressure better than 2×10^{-10} mbar, in the specular geometry ($\theta_i = \theta_f = 45^\circ$), with a primary beam energy of 4 eV and a typical elastic peak resolution of ca. 50 cm^{-1} (6.2 meV fwhm). Spectra were normalized to the elastic peak intensity. Sample preparation was carried out in an adjacent UHV preparation chamber with a base pressure better than 5×10^{-10} mbar, allowing fast transfer between the two chambers and preserving a contamination free environment for HREEL measurements. A maximum likelihood based resolution enhancement method was used to recover the spectra from the instrumental broadening.^{46,47}

X-ray Photoelectron Spectroscopy (XPS). The photoemission studies were performed at the SuperESCA beamline^{48,49} of the Elettra third generation synchrotron radiation source in Trieste, Italy. The experimental chamber was equipped with a Phoibos hemispherical

energy analyzer (SPECS GmbH) with a homemade delay-line detector,⁵⁰ and has a background pressure of about 2×10^{-10} mbar. Core level spectra were recorded with the sample at room temperature and at a photon energy of 320 eV (Au (4f), 400 eV (C (1s)) 500 eV (N (1s)), or 650 eV (O (1s)), with an overall energy resolution of better than 100–250 meV. Core level spectra binding energies were referenced to the Fermi level. XP spectra were used to verify surface cleanliness.

The core level XP spectra were fitted using the CasaXPS commercial fitting package using a Shirley type background and a Gaussian (70%)-Lorentzian (30%) shape function for each emission.

In each chamber, the Au(111) crystal was cleaned by repeated cycles of Ar^+ sputtering at 300 K and annealing at 825–875 K for ~10 min. The sample was then exposed to (S)-proline (SigmaAldrich, ≤99.5%) via sublimation from a solid doser. The temperature of (S)-proline was monitored via a thermocouple. It should be noted that position, distance from sample, and flux each influence the arrival rate of molecules from a solid sublimation doser, we thus varied the sample temperature and deposition times in an attempt to counteract the differences in dosing position and distance in all three chambers. The temperatures used were 350 and 415 K, this accounts for the variance in “exposure” in Langmuirs between experimental chambers. Although

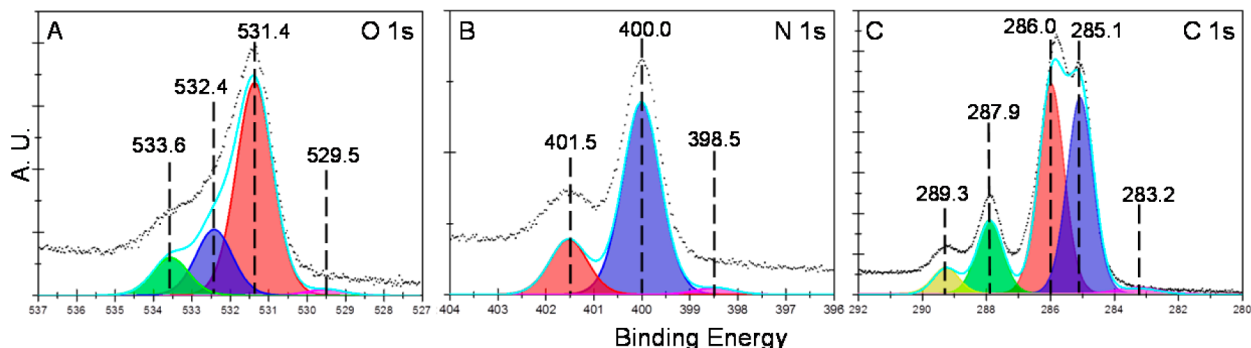


Figure 3. O (1s) (A); N (1s) (B); and C (1s) (C) XP spectra of Au(111) exposed to (S)-proline at 300 K. Spectra were recorded at 300 K at different photon energies: (A) 650 eV; (B) 500 eV; and (C) 400 eV. All spectra were collected normal to the surface.

we cannot be absolutely certain that the same proline coverage was achieved in each experimental apparatus, adsorption at 300 K ensures that submonolayer coverages were achieved, as was reported by Gao et al. on the more reactive Pd(111) surface.²⁶

RESULTS AND DISCUSSION

Scanning Tunneling Microscopy (STM). Figure 2A shows an STM image, acquired at 77 K, of the Au(111) surface after exposure to 0.66 L (S)-proline at 300 K. Approximately 55% of the surface is covered in molecular features. Two distinct island morphologies are observed. The most common morphology consists of 1-D islands of ordered molecular features that are typically a few tens of nanometres in length and a few nanometres in width. The lower half of Figure 2B shows a small area of an ordered island, where some differences in contrast can be observed between features at the center and those at the edges of the islands. The features in the middle of the island are circular in appearance and adopt a close-packed hexagonal arrangement with intermolecular spacings of 5.8 ± 0.1 Å. The features at the island edges are more elongated in appearance. The growth direction of the ordered molecular chains (and the molecular features within the chains) is along the $\langle 0\bar{1}1 \rangle$ -type high symmetry directions. Consequently, the ordered arrangement of molecules is consistent with a commensurate $p(2 \times 2)$ structure. A second island growth morphology can also be observed in Figure 2B. This involves the formation of long islands with less well-defined growth directions than the ordered islands and with a more random molecular arrangement within the islands. As was observed in the cysteine/Au(111) system, the nucleation of islands appears to occur at surface features, such as step edges and the soliton boundaries and elbows of the herringbone reconstruction.³⁹

STM measurements were carried out using low tunneling currents (~ 0.03 nA), as using higher currents (> 0.1 nA) made imaging difficult due to the stronger tip-molecule interactions. This is indicative of a very weakly bound adsorbate and is also consistent with the fact that no ordered structures were observed when scanning at 300 K—merely indications of rapidly diffusing species.

Figure 2C shows the surface after annealing to 340 K and cooling to 77 K. The annealing procedure induces a dramatic change in the surface morphology. Instead of ordered 2-D islands, chains are observed which have a width of two molecular dimensions. The chains are highly mobile, as evidenced by the fact that only a few features appear circular, with the majority being distorted. Consecutive images (not shown) revealed that molecules within the chains are highly

mobile, with chains attaching and detaching from other chains. There was also a high degree of streaking on the images, as molecules were continuously being dragged by the tip. In addition, there is evidence of molecular condensation at step edges. The annealing procedure causes a significant lowering of the surface coverage of proline via thermal desorption. It is difficult to quantify the exact surface coverage due to the mobility of isolated proline species.

Figure 2D shows STM images of the surface after annealing to 370 K and cooling to 77 K. At this stage molecular features can no longer be resolved. The herringbone reconstruction characteristic of the clean Au(111) surface can now be clearly resolved. Some elbows of the herringbone reconstruction were found to contain small islands of unresolvable material.

X-ray Photoelectron Spectroscopy (XPS). Figure 3A–C shows XP spectra obtained for the O (1s), N (1s), and C (1s) core levels following the adsorption of 180 L (S)-proline at 300 K. The O (1s) core level region shown in Figure 3A can be deconvoluted into three main features at binding energies of 531.4, 532.4, and 533.6 eV giving an intensity ratio of $\sim 6:2:1$. In addition, a small shoulder is evident at low binding energy (529.5 eV). Figure 3B shows the N (1s) core level region, which consists of two main peaks at binding energies of 400.0 and 401.5 eV with the lower binding energy peak being approximately four times as intense as the higher binding energy feature. A small feature is also observed at a binding energy of 398.5 eV. Figure 3C shows the C (1s) core level region. The most intense feature is clearly resolvable into two approximately equal contributions from peaks at binding energies of 285.1 and 286.0 eV. Additional smaller peaks are observed at 287.9 and 289.3 eV, and a very weak feature at 283.2 eV. In each of the O (1s), N (1s), and C (1s) XP spectra, a low binding energy feature is observed, corresponding, in each case, to a few percent of the total signal. Similar peaks were reported following proline decomposition on TiO₂(110) by Fleming et al.³² In the present study, we assign these peaks to a low level of proline decomposition presumably at defect sites on the Au surface.

High Resolution Electron Energy Loss Spectroscopy (HREELS). The HREEL spectrum in Figure 4 was acquired at room temperature after exposing Au(111) to 9 L (S)-proline at 300 K. Two main peaks are observed at low frequency, at 480 cm^{-1} and at 755 cm^{-1} . In addition, features are observed at 1030 , 1110 , 1245 , 1390 , 1520 , and 1620 cm^{-1} ; an asymmetric feature which consists of an intense peak at 3015 cm^{-1} with a low frequency shoulder at 2880 cm^{-1} .

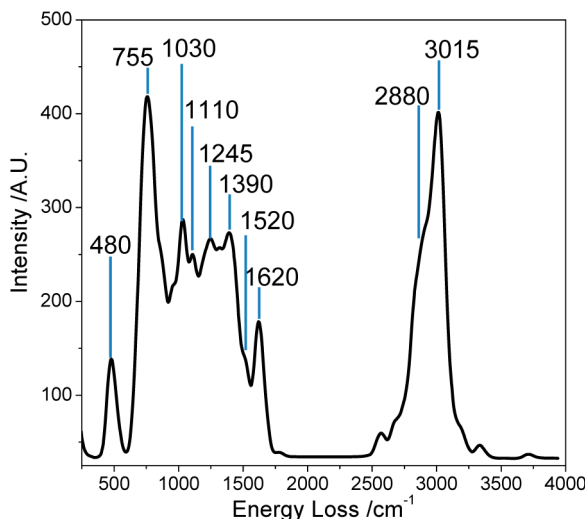


Figure 4. Enhanced HREEL spectrum of the Au(111) sample after exposure to (S)-proline at 300 K. The data were acquired at 300 K.

DISCUSSION

XPS. The adsorption of amino acids onto metal surfaces most commonly occurs via the anionic form (i.e., R-CHNH₂-COO⁻) with a direct bond to the surface involving the N atom and one oxygen atom (μ_2 geometry) or both oxygen atoms (μ_3 geometry).^{7–9,17,19–21,51} The adsorption of proline,²⁶ alanine,²⁷ and glycine²⁸ on Pd(111) and glutamic acid onto Ni(111)²⁹ have been reported to occur via the zwitterionic form of the amino acid (i.e., R-CHNH₃⁺-COO⁻). In this case, the interaction between the surface occurs predominantly via the carboxylate group.^{26–29} The profiles of the C, N, and O (1s) XP spectra in this work are similar to those reported by Jones et al.¹⁵ for a 5-nm thick multilayer of alanine on Cu(110). The absolute binding energies in the work of Jones et al.¹⁵ are

systematically offset by ~1.0–1.5 eV compared with the present work likely as a result of the thick multilayer under investigation. In the N (1s) region, Jones et al.¹⁵ assigned peaks at 401.2 and 403.0 eV to multilayer alanine with the former peak corresponding to neutral (non-zwitterionic) alanine (i.e., R-CHNH₂-COOH) and the latter peak assigned to zwitterionic alanine. The multilayer was considered to consist of a mixture of neutral and zwitterionic species. The N (1s) XP spectrum contains two peaks which can be assigned to the uncharged and protonated amino groups. The binding energy of 401.5 eV is in agreement with the -NH₂⁺ of proline on TiO₂(110) and the larger peak at 400.0 eV is also in agreement with the neutral -NH- species on TiO₂(110).³²

The asymmetric peak seen in the O (1s) XP spectra can be interpreted as consisting of a large peak at 531.4 eV with a shoulder at a higher binding energy, this shoulder can be fitted with two peaks. As such, the two distinct parts of the spectrum—the large peak and the two smaller peaks—represent different types of proline species. The dominant peak is assigned to the isoelectronic oxygen atoms of the carboxylate species (likely to be from proline in the zwitterionic (R-NH₂⁺-COO⁻) and/or anionic (R-NH-COO⁻) form). The peak at highest binding energy relates to the hydroxyl oxygen and the larger peak at 532.4 eV to the carbonyl of the neutral species. A similar assignment is made by Classen et al. for the oxygen atoms in the carboxylic acid functional groups of trimesic acid on Cu(110).³²

The highest binding energy feature in the C (1s) XP spectrum of alanine/Cu(110) was assigned to a carboxylate/carboxylic acid group¹⁵—we make a similar conclusion in this work, although, as in the study of trimesic acid on Cu(110) by Classen et al.,³² it is possible to distinguish between the carboxylic acid (289.3 eV) and the carboxylate (287.9 eV). The two larger peaks correspond to the four carbon atoms of the pyrrolidine ring, the peak at higher binding energy represents C² and C⁵ (see Figure 1) (i.e., those carbons attached to the

Table 1. Assignment of Peaks Observed in the HREELS Experiment of (S)-Proline on Au(111) at 300 K by Comparison with Infrared Data from a Number of Literature Sources

(S)-proline on Au(111) (this work)	zwitterionic proline ⁵⁴	neutral proline ⁵⁵	Cu(II)prolinate ⁵⁴	(S)-proline (KBr pellet)	assignment ^{17,54–56}
		3393–3369		3417	NH stretch
3015	3050	3025	3196–3101	3062	
2880	3006–2875	2984–2846 1795–1766	2978–2873	2985	C _x H _y stretches C=O stretch
1620	1619		1628/1604	1624	OCO asym stretch
1520	1555			1565	NH ₂ scissors
	1472/1447	1488–1451	1450/1441	1447	CH ₂ bend
1390	1402	1412/1405	1418/1397		OCO sym stretch
	1375	1384/1381 1364	1375		NH ₂ twist
	1340/1317	1350/1330	1357/1319	1330	NH bend
	1292/1289	1320	1304	2388	CH ₂ bend
1245	1253/1225	1294–1206	1270/1238		CH ₂ twist
	1168	1150/1142	1186	1169	CH ₂ wag
1110	1083–1051	1109/1105/1072	1096/1079	1088	NH ₂ twist/NH bend
1030	1033–979	1021	1068/1041	1043, 995 847	CH ₂ rock
755				783	CH ₂ wag
480				679, 630 459	NH ₂ rock + CN stretch ⁵⁶ NH ₂ rock + CC stretch ⁵⁶ OCO rock + OCO bend + CN stretch ⁵⁶ OCO rock + OCO bend + CC rock ⁵⁶

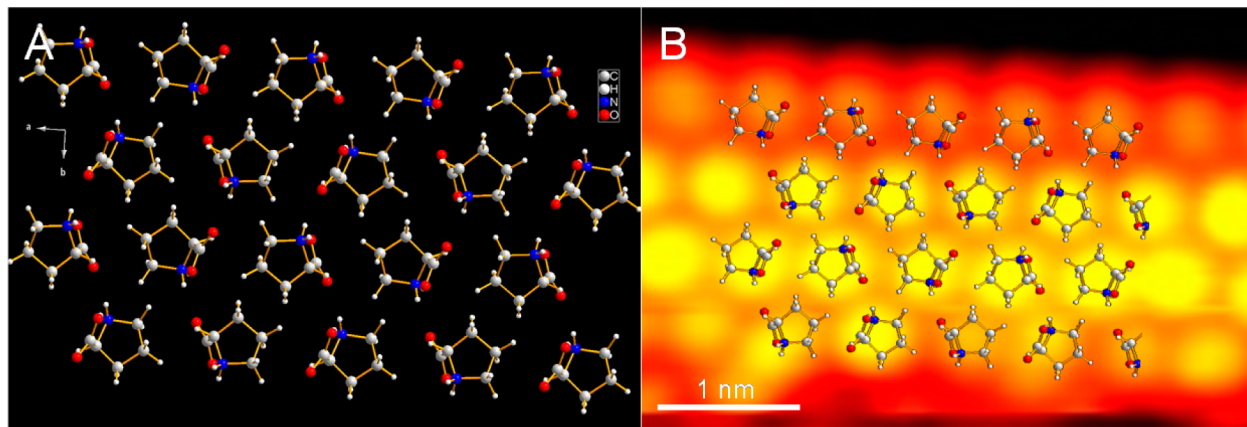


Figure 5. (A) crystal structure of (S)-proline⁶⁰ (a) and crystal structure superimposed onto a portion of an STM image from Figure 2B.

nitrogen atom of the pyrrolidine ring), and the peak at lowest binding energy represents C³ and C⁴. Taking the sum of the areas of the two peaks, which correspond to C¹ (i.e., the peaks at 289.3 and 287.9 eV) and comparing this to the areas of the peak assigned to C³ and C⁴ (285.1 eV) and C² and C⁵ (286.0 eV) yields a ratio of approximately 1:2:2 which would be the expected value if all carbons of the proline molecule are sampled equally. This suggests that there is no preferred orientation of the pyrrolidine ring in the present study, in contrast to the conclusions drawn in the study of proline on TiO₂(110)³² and is to be expected given that proline exists as a 2-D gas at 300 K, the XPS acquisition temperature. Comparing the ratio of the peaks assigned to carboxylic acid versus carboxylate implies that at 300 K, approximately 75% of proline molecules exist in the carboxylate form. The combination of C (1s), N (1s), and O (1s) XP spectra imply that proline exists in a number of forms on Au(111) at 300 K. From the C and O (1s) spectra, it is clear that the majority of proline species contain the carboxylate functionality. However, the N (1s) spectrum implies that the majority of proline species contain the NH functionality with a minority possessing the NH₂⁺ functionality. One possible conclusion is that proline exists as a mixture of the cationic form (R-NH₂⁺-COOH) and the anionic form (R-NH-COO⁻) with the latter species being dominant. It is more physically sensible for proline to exist as a mixture of zwitterionic, neutral (R-NH-COOH) and anionic forms with the anionic form being the most common species (Figure 1). The driving force for formation of the anionic species would likely be the fact that H+H recombination (to produce gas phase H₂), which occurs below room temperature on Au(111),⁵³ depletes the surface of hydrogen favoring the deprotonated species.

HREELS. Table 1 summarizes the vibrational frequencies of bands observed in the HREEL spectrum and their assignments using studies of zwitterionic, neutral proline, and an anionic proline salt for comparison.^{17,54,55} Amino acids tend to exist in the zwitterionic form in the solid state; while in the gas phase, in the absence of intermolecular bonds, the non-zwitterionic form is adopted.⁵⁷ As shown, for example, by studies of the neutral (non-zwitterionic) form of glutamic acid in an argon matrix⁵⁷ and of proline⁵⁸ in the gas phase, the two forms should be readily distinguishable by their vibrational spectra. In the HREEL spectrum displayed in Figure 4, there is no indication of a peak in the 1700–1800 cm⁻¹ range, which would be indicative of a free carbonyl band.⁵⁸ However, there are features at 1390 and 1620 cm⁻¹ which can be assigned to

the symmetric and asymmetric stretches of the carboxylate group.^{16,52,59} This allows two possible conclusions from the HREELS data. Either one may conclude that the only species present are the zwitterionic or anionic forms of proline or, alternatively, the neutral form could be present but the carbonyl group of this species is parallel to the surface and therefore not observed in HREELS due to the metal surface dipole selection rule. The C (1s) XPS data indicate that some carboxylic acid is present on the surface. The STM data indicate that desorption of proline occurs at a relatively low temperature so the interaction between metal and molecule is relatively weak which would imply that surface-molecule interactions are unlikely to produce a well-defined molecular geometry. However, the formation of intermolecular hydrogen bonds may lead to molecular orientations where the carbonyl group is predominantly parallel to the surface. A key difference between the XPS and HREELS experiments is the time scale. It is possible that the non-zwitterion: zwitterion ratio varies with time such that over the longer time scale (~8 h) of the HREELS experiment, the zwitterionic and/or anionic forms become increasingly dominant. The ordered structures observed in STM (acquired at 77 K) exhibit a very similar intermolecular spacing to that observed in the ab plane of solid proline which exists in the zwitterionic form (Figure 5a).⁶⁰ It is likely that the ordered molecular arrangements observed correspond to zwitterionic proline while the more random arrangements of molecules contain a mixture of anionic, zwitterionic and neutral species. The strong similarity between the ordered arrays of proline and the ab plane of zwitterionic (S)-proline is illustrated in Figure 5b where the crystal structure is superimposed onto one such island. On Cu(110), a (2 × 4) structure is produced with two proline molecules (in the anionic form) per unit cell. The nearest neighbor molecular spacing is significantly larger (6.26 Å) than we find for proline on Au(111)—nearest neighbor spacing 5.8 Å. The more densely packed structure is consistent with relatively favorable ionic intermolecular interactions expected for the zwitterionic species. The STM image of Figure 2A shows a mixture of ordered regions, which we believe are made up of primarily zwitterionic proline species and disordered regions, which the spectroscopic measurements imply are likely to be a mixture of species. The proportion of zwitterionic species observed in STM measurements is apparently higher than that observed spectroscopically (at 300 K)—although it is important to add the note of caution that STM is very much a local probe. This adds further weight to the idea that dehydrogenation processes

occur readily at 300 K, but are quenched by cooling the sample to 77 K.

CONCLUSIONS

Proline is able to adsorb onto Au(111) at 300 K forming ordered molecular structures on cooling to 77 K, which nucleate at surface defects such as step edges and soliton boundaries of the herringbone reconstruction. The adsorbed proline interacts only weakly with the Au surface—a submonolayer coverage of proline desorbs almost completely by 370 K. XPS indicates that proline exists as a mixture of the neutral, zwitterionic, and anionic forms, though HREELS experiments were only able to detect the zwitterionic and anionic forms. It is proposed that over the time scale of the HREELS experiments, the neutral form is able to deprotonate with the driving force being the facile liberation of H₂ into the gas phase. The dimensions of the ordered structures observed are consistent with the formation of a 2-D analogue of the 3-D crystal structure of proline (which exists in the zwitterionic form in the solid state). In the 77 K STM experiments, there is a coexistence of ordered and disordered molecular regions. We speculate that the disordered regions consist of a random mixture of the neutral, zwitterionic, and anionic forms of proline.

AUTHOR INFORMATION

Corresponding Author

*E-mail: cjb14@st-and.ac.uk.

Notes

The authors declare no competing financial interest.

ACKNOWLEDGMENTS

R.T.S.G. and J.G. acknowledge the Engineering and Physical Sciences Research Council (EPSRC, U.K.) for the award of a PhD studentship. The research leading to these results has received funding from the European Community's Seventh Framework Programme (FP7/2007-2013) under Grant Agreement No. 312284.

REFERENCES

- (1) Rosi, N. L.; Mirkin, C. A. Nanostructures in Biodiagnostics. *Chem. Rev.* **2005**, *105*, 1547.
- (2) Joachim, C.; Gimzewski, J. K.; Aviram, A. Electronics Using Hybrid-Molecular and Mono-Molecular Devices. *Nature* **2000**, *408*, 541.
- (3) Romaner, L.; Heimel, G.; Gruber, M.; Brédas, J.-L.; Zoyer, E. Stretching and breaking of a molecular Junction. *Small* **2006**, *2*, 1468.
- (4) Lausmaa, J.; Löfgren, P.; Kasemo, B. Adsorption and Coadsorption of Water and Glycine on TiO₂. *J. Biomed. Mat. Res.* **1999**, *44*, 227.
- (5) Fleming, G. J.; Adib, K.; Rodriguez, J. A.; Barreau, M. A.; White, J. M.; Idriss, H. The Adsorption and Reactions of the Amino Acid Proline on Rutile TiO₂(110) Surfaces. *Surf. Sci.* **2008**, *602*, 2029.
- (6) Izumi, Y. Modified Raney-Nickel (MRNi) Catalyst-Heterogeneous Enantio-Differentiating (Asymmetric) Catalyst. *Adv. Catal.* **1983**, *32*, 215.
- (7) Barlow, S. M.; Kitching, K. J.; Haq, S.; Richardson, N. V. A Study of Glycine Adsorption on a Cu{110} Surface Using Reflection Absorption Infrared Spectroscopy. *Surf. Sci.* **1998**, *401*, 322.
- (8) Kang, J. H.; Toomes, R. L.; Polcik, M.; Kittel, M.; Hoeft, J. T.; Efsthathiou, V.; Woodruff, D. P.; Bradshaw, A. M. Structural Investigation of Glycine on Cu(100) And Comparison to Glycine on Cu(110). *J. Chem. Phys.* **2003**, *118*, 6059.
- (9) Chen, Q.; Frankel, D. J.; Richardson, N. V. Chemisorption Induced Chirality: Glycine on Cu{110}. *Surf. Sci.* **2002**, *497*, 37.
- (10) Nyberg, M.; Hasselstrom, J.; Karis, O.; Wassdahl, N.; Weinelt, M.; Nilsson, A.; Pettersson, L. G. M. The Electronic Structure and Surface Chemistry of Glycine Adsorbed on Cu(110). *J. Chem. Phys.* **2000**, *112*, 5420.
- (11) Toomes, R. L.; Kang, J. H.; Woodruff, D. P.; Polcik, M.; Kittel, M.; Hoeft, J. T. Can Glycine Form Homochiral Structural Domains on Low-Index Copper Surfaces? *Surf. Sci.* **2003**, *522*, L9.
- (12) Sayago, D. I.; Polcik, M.; Nisbet, G.; Lamont, C. L. A.; Woodruff, D. P. Local Structure Determination of a Chiral Adsorbate: Alanine on Cu(110). *Surf. Sci.* **2005**, *590*, 76.
- (13) Rankin, R. B.; Sholl, D. S. Structures of Glycine, Enantiopure Alanine, and Racemic Alanine Adlayers on Cu(110) And Cu(100) Surfaces. *J. Phys. Chem. B* **2005**, *109*, 16764.
- (14) Cheong, W. Y.; Huang, Y.; Dangaria, N.; Gellman, A. J. Probing Enantioselectivity on Chirally Modified Cu(110), Cu(100), and Cu(111) Surfaces. *Langmuir* **2010**, *26*, 16412.
- (15) Jones, G.; Jones, L. B.; Thibault-Starzyk, F.; Seddon, E. A.; Raval, R.; Jenkins, S. J.; Held, G. The Local Adsorption Geometry and Electronic Structure of Alanine on Cu{110}. *Surf. Sci.* **2006**, *600*, 1924.
- (16) Williams, J.; Haq, S.; Raval, R. The Bonding and Orientation of the Amino Acid L-Alanine on Cu{110} Determined by RAIRS. *Surf. Sci.* **1996**, *368*, 303.
- (17) Marti, E. M.; Barlow, S. M.; Haq, S.; Raval, R. Bonding and Assembly of the Chiral Amino Acid S-Proline on Cu(110): The Influence of Structural Rigidity. *Surf. Sci.* **2002**, *501*, 191.
- (18) Shavorskiy, A.; Aksoy, F.; Grass, M. E.; Liu, Z.; Bluhm, H.; Held, G. A Step toward the Wet Surface Chemistry of Glycine and Alanine on Cu{110}: Destabilization and Decomposition in the Presence of Near-Ambient Water Vapor. *J. Am. Chem. Soc.* **2011**, *133*, 6659.
- (19) Barlow, S. M.; Louafi, S.; Le Roux, D.; Williams, J.; Muryn, C.; Haq, S.; Raval, R. Supramolecular Assembly of Strongly Chemisorbed Size- and Shape-Defined Chiral Clusters: S- and R-Alanine on Cu(110). *Langmuir* **2004**, *20*, 7171.
- (20) Eralp, T.; Shavorskiy, A.; Zheleva, Z. V.; Held, G.; Kalashnyk, N.; Ning, Y. X.; Linderoth, T. R. Global and Local Expression of Chirality in Serine on the Cu{110} Surface. *Langmuir* **2010**, *26*, 18841.
- (21) Eralp, T.; Shavorskiy, A.; Held, G. The Adsorption Geometry and Chemical State of Lysine on Cu{110}. *Surf. Sci.* **2011**, *605*, 468.
- (22) Humblot, V.; Methivier, C.; Raval, R.; Pradier, C. M. Amino Acid and Peptides on Cu(110) Surfaces: Chemical and Structural Analyses of L-Lysine. *Surf. Sci.* **2007**, *601*, 4189.
- (23) Kim, J. W.; Lee, Y. M.; Lee, S. M.; Son, M. J.; Kang, H.; Park, Y. Surface Reaction of Sulfur-Containing Amino Acids on Cu(110). *Langmuir* **2010**, *26*, 5632.
- (24) Feyer, V.; Plekan, O.; Skála, T.; Cháb, V.; Matolín, V.; Prince, K. C. The Electronic Structure and Adsorption Geometry of L-Histidine on Cu(110). *J. Phys. Chem. B* **2008**, *112*, 13655.
- (25) Mateo Marti, E.; Methivier, C.; Pradier, C. M. (S)-Cysteine Chemisorption on Cu(110), from the Gas or Liquid Phase: An FT-RAIRS and XPS Study. *Langmuir* **2004**, *20*, 10223.
- (26) Gao, F.; Wang, Y. L.; Burkholder, L.; Tysoe, W. T. Chemistry of L-Proline on Pd(111): Temperature-Programmed Desorption and X-ray Photoelectron Spectroscopic Study. *Surf. Sci.* **2007**, *601*, 3579.
- (27) Gao, F.; Li, Z. J.; Wang, Y. L.; Burkholder, L.; Tysoe, W. T. Chemistry of Alanine on Pd(111): Temperature-Programmed Desorption and X-ray Photoelectron Spectroscopic Study. *Surf. Sci.* **2007**, *601*, 3276.
- (28) Gao, F.; Li, Z. J.; Wang, Y. L.; Burkholder, L.; Tysoe, W. T. Chemistry of Glycine on Pd(111): Temperature-Programmed Desorption and X-ray Photoelectron Spectroscopic Study. *J. Phys. Chem. C* **2007**, *111*, 9981.
- (29) Jones, T. E.; Urquhart, M. E.; Baddeley, C. J. An Investigation of the Influence of Temperature on the Adsorption of the Chiral Modifier, (S)-Glutamic Acid, on Ni{111}. *Surf. Sci.* **2005**, *587*, 69.
- (30) Trant, A. G.; Baddeley, C. J. Surface Chemistry Underpinning Enantioselective Heterogeneous Catalysis: Supramolecular Self-

- Assembly of Chiral Modifiers and Pro-Chiral Reagents on Ni{111}. *J. Phys. Chem. C* **2011**, *115*, 1025.
- (31) Wilson, K. E.; Baddeley, C. J. XPS Studies of the Effects of Modification Ph on the Interaction of Methylacetoacetate with (S)-Aspartic Acid-Modified Ni Surfaces. *J. Catal.* **2011**, *278*, 41.
- (32) Fleming, G. J.; Adib, K.; Rodriguez, J. A.; Barreau, M. A.; Idriss, H. Proline Adsorption on TiO₂(110) Single Crystal Surface: A Study by High Resolution Photoelectron Spectroscopy. *Surf. Sci.* **2007**, *601*, 5726.
- (33) Qiu, T.; Barreau, M. A. STM Study of Glycine on TiO₂(110) Single Crystal Surfaces. *J. Colloid Interface Sci.* **2006**, *303*, 229.
- (34) Thomas, A. G.; Flavell, W. R.; Chatwin, C. P.; Kumarasinghe, A. R.; Rayner, S. M.; Kirkham, P. F.; Tsoutsou, D.; Johal, T. K.; Patel, S. Adsorption of Phenylalanine on Single Crystal Rutile TiO₂(110) Surface. *Surf. Sci.* **2007**, *601*, 3828.
- (35) Tonner, R. Adsorption of Proline and Glycine on the TiO₂(110) Surface: A Density Functional Theory study. *ChemPhysChem* **2010**, *11*, 1053.
- (36) Ataman, E.; Isvoranu, C.; Knudsen, J.; Schulte, K.; Andersen, J. N.; Schnadt, J. Adsorption of L-Cysteine on Rutile TiO₂(110). *Surf. Sci.* **2011**, *605*, 179.
- (37) De Renzi, V.; Lavagnino, L.; Corradini, V.; Biagi, R.; Canepa, M.; del Pennino, U. Very Low Energy Vibrational Modes as a Fingerprint of H-Bond Network Formation: L-Cysteine on Au(111). *J. Phys. Chem. C* **2008**, *112*, 14439.
- (38) Nazmutdinov, R. R.; Manyurov, I. R.; Zinkicheva, T. T.; Jang, J.; Ulstrup, J. Cysteine Adsorption on the Au(111) Surface and the Electron Transfer in Configuration of a Scanning Tunneling Microscope: A Quantum-Chemical Approach. *Russ. J. Electrochem.* **2007**, *43*, 328.
- (39) Mateo-Martí, E.; Rogero, C.; Gonzalez, C.; Sobrado, J. M.; de Andrés, P. L.; Martin-Gago, J. A. Interplay between Fast Diffusion and Molecular Interaction in the Formation of Self-Assembled Nanostructures of S-Cysteine on Au(111). *Langmuir* **2010**, *26*, 4113.
- (40) Naitabdi, A.; Humblot, V. Chiral Self-Assemblies of Amino-Acid Molecules: D- and L-Methionine on Au(111) Surface. *Appl. Phys. Lett.* **2010**, *97*, 223112.
- (41) Zhao, X. Y.; Yan, H.; Zhao, R. G.; Yang, W. S. Physisorption-Induced Surface Reconstruction and Morphology Changes: Adsorption of Glycine on the Au(110) 1 × 2 Surface. *Langmuir* **2002**, *18*, 3910.
- (42) Wilson, K. E.; Frücht, H. A.; Grillo, F.; Baddeley, C. J. (S)-Lysine Adsorption Induces the Formation of Gold Nanofingers on Au{111}. *Chem. Commun.* **2011**, *47*, 10365.
- (43) Forster, M.; Dyer, M. S.; Persson, M.; Raval, R. Probing Conformers and Adsorption Footprints at the Single-Molecule Level in a Highly Organized Amino Acid Assembly of (S)-Proline on Cu(110). *J. Am. Chem. Soc.* **2009**, *131*, 10173.
- (44) Forster, M.; Dyer, M. S.; Persson, M.; Raval, R. 2D Random Organization of Racemic Amino Acid Monolayers Driven by Nanoscale Adsorption Footprints: Proline on Cu(110). *Angew. Chem., Int. Ed.* **2010**, *49*, 2344.
- (45) Forster, M.; Dyer, M. S.; Persson, M.; Raval, R. Assembly of Chiral Amino-Acids at Surfaces from a Single Molecule Perspective: Proline on Cu(110). *Top. Catal.* **2011**, *54*, 13.
- (46) Frederick, B. G.; Nyberg, G. L.; Richardson, N. V. Spectral Restoration in Herels. *J. Electron Spectrosc. Relat. Phenom.* **1993**, *64–5*, 825.
- (47) Frederick, B. G.; Richardson, N. V. Ultrahigh-Resolution Electron-Energy-Loss Spectroscopy—Comment. *Phys. Rev. Lett.* **1994**, *73*, 772.
- (48) Baraldi, A.; Comelli, G.; Lizzit, S.; Kiskinova, M.; Paolucci, G. Real-Time X-ray Photoelectron Spectroscopy of Surface Reactions. *Surf. Sci. Rep.* **2003**, *49*, 169.
- (49) Baraldi, A.; Barnaba, M.; Brena, B.; Cocco, D.; Comelli, G.; Lizzit, S.; Paolucci, G.; Rosei, R. Time Resolved Core Level Photoemission Experiments with Synchrotron Radiation. *J. Electron. Spectrosc. Relat. Phenom.* **1995**, *76*, 145.
- (50) Cautero, G.; Sergio, R.; Stebel, L.; Lacovic, P.; Pittana, P.; Predonzani, M.; Carrato, S. A Two-Dimensional Detector for Pump-and-Probe and Time Resolved Experiments. *Nucl. Instr. Meth. A* **2008**, *595*, 447.
- (51) Humblot, V.; Methivier, C.; Pradier, C. M. Adsorption of L-Lysine on Cu(110): A RAIRS Study from UHV to the Liquid Phase. *Langmuir* **2006**, *22*, 3089.
- (52) Classen, T.; Lingenfelder, M.; Wang, Y.; Chopra, R.; Virojanadara, C.; Starke, U.; Costantini, G.; Fratesi, G.; Fabris, S.; de Gironcoli, S.; Baroni, S.; Haq, S.; Raval, R.; Kern, K. Hydrogen and Coordination Bonding Supramolecular Structures of Trimesic Acid on Cu(110). *J. Phys. Chem. A* **2007**, *111*, 12589.
- (53) Okada, M.; Nakamura, M.; Moritani, K.; Kasai, T. Dissociative Adsorption of Hydrogen on Thin Au Films Grown on Ir{111}. *Surf. Sci.* **2003**, *523*, 218.
- (54) Herlinger, A. W.; Long, T. V. Laser-Raman and Infrared Spectra of Amino Acids and Their Metal Complexes. III. Proline and Bisprolinato Complexes. *J. Am. Chem. Soc.* **1970**, *92*, 6481.
- (55) Reva, I. D.; Stepanian, S. G.; Plokhotnichenko, A. M.; Radchenko, E. D.; Sheina, G. G.; Blagoi, Y. P. Infrared Matrix Isolation Studies of Amino Acids. Molecular Structure of Proline. *J. Mol. Struct.* **1994**, *318*, 1.
- (56) Wagner, C. C.; Torre, M. H.; Baran, E. J. Vibrational Spectra of Copper(II) Complexes of L-Proline. *Lat. Am. J. Pharm.* **2008**, *27*, 197.
- (57) Navarrete, J. T. L.; Bencivenni, L.; Ramondo, F.; Hernandez, V.; Ramirez, F. J. Structural and Spectroscopic Study of Glutamic-Acid in the Non-Zwitterionic Form. *Theochem.-J. Mol. Struct.* **1995**, *330*, 261.
- (58) Cappelli, C.; Monti, S.; Rizzo, A. Effect of the Environment on Vibrational Infrared and Circular Dichroism Spectra of (S)-Proline. *Int. J. Quantum Chem.* **2005**, *104*, 744.
- (59) Lopez, A.; Heller, T.; Bitzer, T.; Richardson, N. V. A Vibrational Study of the Adsorption of Glycine on Clean and Na Modified Si (100)-2 × 1 Surfaces. *Chem. Phys.* **2002**, *277*, 1.
- (60) Kayushina, R. L.; Vainshtein, B. K. Crystal Structure of (S)-Proline. *Cryst. Rep.* **1965**, *10*, 833.